Oligonucleotide probes functionalization of nano-gap electrodes

Rosa Letizia Zaffino[1,3*], Mònica Mir[1,2*], Josep Samitier[1,2,3]

[1]Nanobioengineering group, Institute for Bioengineering of Catalonia (IBEC), Baldiri Reixac 10-12, 08028 Barcelona, Spain

[2]Centro de Investigación Biomédica en Red en Bioingeniería, Biomateriales y Nanomedicina (CIBER-BBN), Spain.

[3] Department of Engineering: Electronics, University of Barcelona, C/ Martí i Franqués 1, 08028, Barcelona, Spain

Corresponding authors*: Dr. Monica Mir, Baldiri reixac, 10-12, 08028, Barcelona, Spain, mmir@ibecbarcelona.eu. Dr. Rosa Letizia Zaffino, Instituto de Microelectrónica de Barcelona IMB-CNM-CSIC, Campus Univ. Autónoma de Barcelona, 08193, Bellaterra, Barcelona, Spain, rossella.zaffino@imb-cnm.csic.es

Abbreviations; Desoxyribonucleic acid (DNA), self-assembled monolayers (SAM), focused ion beam (FIB), single nucleotide polymorphisms (SNP), working electrode (WE), reference electrode (RE), counter electrode (CE), oligo-probe (OP), silicon-on-insulator (SOI), double deionized water (DDI), scanning electron microscopy (SEM), Tris (2-carboxylethyl) phosphine hydrochloride (TCEP), cyclic voltammetry (CV), direct current (DC).

Received: 12 16, 2016; Revised: 04 24, 2017; Accepted: 04 24, 2017

This article has been accepted for publication and undergone full peer review but has not been through the copyediting, typesetting, pagination and proofreading process, which may lead to differences between this version and the Version of Record. Please cite this article as doi: 10.1002/elps.201600554 .

Keywords; Nano-gap electrodes, site-selective deposition, biosensor bioelectronics, DNA electrophoresis, self-assembled monolayers (SAM), nanotechnology

Number of words; 6516

Abstract

Nano-gap electrodes have attracted a lot of consideration as promising platform for molecular electronic and biomolecules detection. This is mainly for their higher aspect ratio, and because their electrical properties are easily accessed by current-voltage measurements. Nevertheless, application of standard current-voltages measurements used to characterize nano-gap response, and/or to modify specific nano-gap electrodes properties, represents an issue. Since the strength of electrical fields in nano-scaled devices can reach high-values, even at low voltages.

Here, we analyzed the effects induced by different methods of surface modification of nano-gap electrodes, in test-voltage application, employed for the electrical detection of a DNA target. Nano-gap electrodes were functionalized with two anti-symmetric oligo probes designed to have 20 terminal bases complementary to the edges of the target, which after hybridization bridges the nano-gap, closing the electrical circuit. Two methods of functionalization were studied for this purpose; a random self-assembling of a mixture of the two oligo-probes used in the platform, and a selective method that controls the position of each oligo-probe (OP) at selected side of nano-gap electrodes. We used for this aim, the electrophoretic effect induced on negatively charged probes by the application of an external DC voltage.

The results obtained with both functionalization methods where characterized and compared in terms of electrode surface covering, calculated by using voltammetry analysis.

Moreover, we contrasted the electrical detection of a DNA target in the nano-gap platform either in site-selective and in randomly assembled nano-gap. According our results, a denser, although not selective surface functionalization, is advantageous for such kind of applications.

1. Introduction

The rapid advances of nano-fabrication processing with the increased ability to manipulate nano-scaled systems and materials prompted the development of electronic devices, which include different type of nano-probes. Nano-probes such as nanowires, nanotubes and nanoparticles are used either for signal enhancement in biosensors [1], and in more general molecular electronics applications.

The improved physical-chemical properties and higher aspect ratio of nano-probes and nano-materials increase detection's performances of biosensors [2]. Compared to other available nano-probes, nano-gap electrodes provide some fruitful advantages for biomolecules detection, which motivate the raising interest in their use [3]. By definition, a nano-gap is formed by two metallic electrodes which are separated by an insulating gap (usually air) of nano-metric thickness. Their size can be adjusted to fit that of molecules or biomolecules to analyze, such that their properties, once trapped between the electrodes, can be obtained by monitoring the change induced in nano-gaps electrical response.

Current lithography technologies allow the fabrication of nano-gaps with variable sizes and design in the range between ten and hundreds of nanometers, bounded from below by spot size of electrons (or ions) beam used in nano-lithography processes, such as in e-beam or focused ion beam (FIB) lithography. Standard photolithography can be then

used to embed nano-gaps inside an electrical circuit, as well as to build interface with customable microfluidics to provide easy integration with the detection units.

The capacity of DNA to self-assemble in controlled nano-metric blocks on gold surface by means of thiol linking made it possible to explore nano-gap ability to transduce specific biomolecular interactions into digital signal useful for the direct electrical detection of DNA. Nano-gap electrodes arranged whether in planar [4] and vertical geometry [5] were used to develop DNA biosensors with selectivity for single nucleotide polymorphisms (SNP) at target concentrations as low as 10 fM. Although, controlled manipulation of molecules within the experimental systems is a major issue for molecular electronic applications. This is still more critical for biomolecules detection, where the efficiency of the recognition layer plays a dominant role.

On a micrometric scale, specific patterning of biomolecules on interdigitated arrays has been shown by photolithography with biocompatible polymers [6]. Also, micro-contact printing techniques have been successfully applied to pattern different biological materials. Among these, polymers, DNA, proteins and cells were patterned on different substrates [7]. Further development in this field such as dip-pen nanolithography enables the functionalization with nano-metric definition of molecules, thanks to the capillary transport at an AFM tip [8]. Regardless the helpfulness, such methods are not compatible with all molecules and are difficult to implement for surfaces exposed on vertical electrodes separated by nano-metric distances, as in the case we consider.

The electrophoretic effect induced on charged probes by an external electrical field has been largely explored in DNA and protein microarrays, to overcome limitations inherent within existing methods of addressing biomolecules at a specific test-site [9]. The selective tuning of an electrical field at a given electrode spot affords to gain control over the

transport and the concentration of oligo-probes at the selected sensor surface. Functionalization of electrode surface assisted by a DC positive bias, permits to select the electrode where is desired to attach a specific DNA bioreceptor in an array and to reduce drastically the hybridization times, from hours to seconds of such DNA biosensors platforms [10]. Beyond application in DNA microarrays, DNA electrophoresis was also explored to realize molecule-electrode junctions employed to study molecular electron transport [11]. This technique provides a versatile template for circuit's patterning of nano-scale electrical devices, thanks to self-assembly and auto-recognizing of complementary base-pairs.

Electrostatic trapping of dsDNA between nano-gap electrodes was also used to analyze the mechanisms of charge transport of either DNA molecules [12], and of the nanowires obtained after metallization of DNA scaffold connecting a nano-gap [13]. Similarly, electrostatic trapping was applied to bridge nano-gaps with dsDNA molecules [10, 14], and DNA's origami [15]. Electrophoretic driving of DNA in nano-gap platforms requires the use of voltages, either for analysis of their properties and to functionalize them for specific applications. Such low applied voltages are enhanced by nano-scaled structures and materials and results in high field strength, which constitute an issue for their utilization. It should be also considered that the functionalization of biomolecules at such nanometric proximity could affect the integrity of the bio-receptors used.

To approach this problem, we analyzed different surface functionalization methods in nano-gap electrodes based device, useful for both bioelectronics and biosensing applications. This platform consist of two faced gold nano-electrodes separated by a 50 nm gap, referred as working electrodes (WEs) and two pseudo-reference (RE) and counter electrode (CE), provided in the near proximity of the nano-gap for different purposes; the electrical manipulation inside the nano-gap of two different DNA oligo probes (OP1,

OP2), for the electrochemical characterization of the system and for the target test-voltage. The array conceived has a versatile design for the easy integration of both electrical and electrochemical interface, which are involved in the experimental set-up (Figure 1). The array of nano-gap electrodes was fabricated by combining standard photolithographic techniques with FIB nano-lithography. All the circuitry patterning but the micro-pads and electrodes, were protected by a layer of SiO_2, which prevents against undesired electrical conduction and reduces the absorption of molecules outside the gold nano-gaps. The result was a multi-layered material alternating, (from the top) 45 nm SiO_2, 70 nm Au and 30 nm Ti on a 500 µm silicon-on-insulator (SOI) wafer. The nano-gap was opened by FIB in this multilayer material, obtaining two faced gold electrodes distance by a 50 nm gap. The functionalization of these electrodes with OP1 and OP2 was performed by two methods; random self-assembling of a mixture of the two OPs and selective immobilization by means of DC bias to specifically attract the OP of interest in each electrode of the gap. Surface coverage of the probes was evaluated by involving electrochemical analysis. The efficacy of the attached capture probe for the hybridization of a complementary target was checked with the nano gap platform with a test-voltage.

2. Materials and Methods

2.1 Materials

Double-polished, silicon dioxide (SiO_2) coated, n-type Si (100) wafers metalized with 30 nm of Ti and 70 nm of Au were obtained from the Institute of Microelectronic of Barcelona (IBM-CNM). All the reagents were purchased at Sigma-Aldrich (Poole, UK) unless otherwise stated, and used as received.

The oligo-probes used in the experiments are thiol terminated ssDNA, 53 bases length, antisymmetric each other, provided by Sigma-Aldrich (Poole, UK).

The sequences are:

OP1:

5'-CTTGAGGAGACGGAACGAAGGGCGTGAAGTGGTGAGGAGTGGTGAAGTGCGGG-3'–Thiol-(C3-S-S),

and OP2:

5'-Thiol-(C6-S-S)-
GGGCGTGAAGTGGTGAGGAGTGGTGAAGTGCGGGCGTCCAGACCGACTGAGCC-3'.

The ssDNA target which is end-to-end complementary to the oligo-probes has the following sequence:

5'- Thiol-(C6-S-S)-
TTCGTTCCGTCTCCTCAAGGGGAAGGCGCGAAGGTGCGTGAG-
GAAGTGAAGGCGTGAAGGCGTGTGAAGGCGGTGGTGCGAAGAGAAGGGGGCTCAGT

CGGTCTGGACG-3'

All reagents were dissolved in double deionized water (DDI), purified with the Millipore A10 Q-gard 1 system (18.2 MΩ.cm at 25^0C), and autoclaved before their use in experiments.

2.3. Fabrication of nano-gap electrodes arrays

Electrodes patterning was obtained through standard photolithography. For this purpose, a SOI wafer, metalized with 10 nm Ti and 70 nm Au, was spin-coated with the reversal photoresist AZ5214 following the three-steps protocol provided by the supplier (Clariant GmbH-Germany). Thereafter, it was exposed through a chromium mask to UV light in

the Mask Aligner MJB, SUSS Microtec. The intensity and duration of the light exposure were respectively 26,5 mW/cm^2 and 7,2 s. According provider's indications the wafer was then immersed for 25 s in the AZ develop. Non-patterned areas were etched in a chemical bath by immersing the substrate in Gold Etchant Type TFA (Transene Company, inc. Danvers) having a rate of 2.8 nm/s. The underlying titanium layer was wet-etched by soaking the wafer for 6 s in a hot solution of TFTN (Transene Company, inc.) accounted by considering that the etching rate at 85 ^{0}C is 50 Å/s. Withdrawal of the protective resist was finally achieved by immersing the sample in the AZ 100 Remover for about 1 min. A second photolithography was done to passivate all the gold wiring but the pads. Then, a layer of SiO_2 with a thickness of 45 nm was evaporated on the substrate and characterized by ellipsometry. The pads were thereafter opened for electrical connection by a lift-off process. In order of achieving nano-gaps with sizes varying from 40 nm to 50 nm, we used a FIB of Ga+ from a Strata DB235 FEI FIB/SEM, operating at an accelerating voltage of 30 kV. As a result, two opposite gold surfaces were obtained after FIB milling. The resulting nano-gaps sizes were characterized by scanning electron microscopy (SEM). The nano-gap electrodes array was then cleaned in oxygen plasma to remove any organic residuals from the fabrication process.

2.4. Random self-assembling of OPs mixture on nano-gap electrodes

Probe oligonucleotides are self- assembled at the electrode gold surface by a dative binding between the thiol groups of the DNA linker and the gold atoms in the electrodes. This process gives rise to self-assembling monolayers that are robust against desorption, oxidation, and reduction over a wide range of potentials. In order to have the thiol groups ready to interact with gold a reduction of the disulfide of thiols groups, which can eventually be formed during long-term storage, was performed. For this purpose, a 0.05 µM solution of either one of the OPs (OP1 or OP2) in 10 mM of TRIS, 1 M of NaCl, 5 mM

of $MgCl_2$, and 1 mM of EDTA at pH 7.5, was added to a 1μM solution of Tris (2-carboxylethyl) phosphine hydrochloride (TCEP) with a volume ratio of 1:200 and mixed for 50 minutes at 55^0C in the Thermomixer Compact of Eppendorf. Once the OPs are ready to use, a solution comprising 0.05 μM of OP1 and OP2 with 0.45 μM of mercapto-hexanol for spacing the probes in 10 mM of TRIS, 1 M of NaCl, 5 mM of $MgCl_2$, and 1 mM of EDTA at pH 7.5 was added to the nano-gap sensor, which was left to incubate overnight. The modified nano-gaps were then thoroughly rinsed and dried with N_2 to remove the non-attached probes before electrical measurements were performed.

2.5. Site selective deposition of DNA on nano-gap electrodes by electrophoretic driving

The reduction of thiol groups in the DNA was performed in the same way as in the random deposition method (section 2.4). A droplet of 20 μl of OP1 (or OP2) solution was then spotted on the nano-gap during the application of a DC signal of 1V for 1 minute, provided by the waveform Generator ww5061 of Tabor Electronics. The signal was applied between the WE1 (or WE2) and the CE of the nano-gap, in such a way to have positive charges accumulated on the WEs chosen for the immobilization of the OPs. Thereafter, the OP solution was rapidly removed by rinsing with PBS solution, which strips away unbound molecules, followed by copious rinsing with DDI water, and dried under a gentle argon flow. The process has been repeated by inverting the role of the WEs to achieve the immobilization of the second OP.

2.6. Target DNA hybridization in the nano-gap

After OP functionalization and characterization, target DNA was hybridized with the immobilized probes attached on the sides of the nano-gap. For this purpose, 1 μM of the target sequence in the hybridization buffer (250 mM of sodium phosphate, 15 mM of

sodium citrate, 150 mM of NaCl, 1 mM of EDTA and 0,02 mM of Triton at pH 7.42) was deposited on the electrodes and left to incubate for 1 h. The hybridized nano-gaps were then thoroughly rinsed and dried with N_2 to remove the non-attached targets before electrical measurements were performed.

2.7. Optical Characterization

2.7.1 Optical Microscopy

Optical microscopy characterization was done by using the microscope by Nikon Instrument Inc. model Eclipse L150.

2.7.2. Scanning Electron Microscopy (SEM)

Imaging of the nano-gap electrodes system was performed with a field emission Microscope NOVA NANOSEM 230 by FEI, operating at an accelerating voltage of 10 kV. High-resolution pictures of empty nano-gaps were taken thereafter fabrication and standard cleaning procedure. The sizes of fabricated nano-gaps were evaluated using the free-software Image J.

2.8. Electrochemical Characterization

To characterize the OPs immobilization on the WEs surfaces we used cyclic voltammetry (CV), which were carried out with the VMP2 Multipotentiostat of Princeton Applied Research. Prior to electrochemical measurements of bare nano-gaps, the array was subjected to a lukewarm bath of piranha solution (3:1 H_2SO_4:H_2O_2) for 1 minute, rinsed with ethanol, acetone and dried with a flow of N_2. The treatment with piranha, which is a strong oxidizing agent, a part to remove organic matter residuals, induces a hydrophilic state on SiO_2, through the formation of OH groups on its surface, enhancing nano-gap

hydrophilicity which facilitates the further delivering of the testing solutions. Electrodes connections were performed with a micro-positioning. CV measurements were done, at room temperature, in a solution obtained by mixing 5 mM of $K_3[Fe(CN)_6]$ and 5 mM of $K_4[Fe(CN)_6]*3.H_2O$ in 0.1 M KCl. A 20 µl droplet of this redox solution was spotted on the nano-gap region to allow CV measurements. After each experiment, it was cleaned and substituted with a fresh one by rinsing with abundant DDI water and drying under argon flow. CVs were recorded by cycling the WE between 0.6 V and -0.6 V vs RE, at a scan rate of 50 mV/s. We limited the analysis to this potential range because cycling at higher redox potentials could result in gold etching from the WE surface, and in the reduction of the thiol bond attached to the gold WEs. We observed stabilization of the voltagram right after completing the first redox cycle, so that we retained that a number of three redox cycles was sufficient to complete the characterization, being the last cycle used for results comparison. This process was fast enough to assure both the integrity of the redox solution under light exposure, and the maintenance of the initial volume of liquid against evaporation. Data treatment was done by using the Software EC-Lab V10.34.

2.9. Electrical Characterization.

Electrical measurements were performed at room atmospheric conditions by using a Keithley sub-femtoAmp Remote Source meter, Model 6430 (Keithley inc.) which combines a precise stable DC power supply within a high-impedance multimeter and a remote amplifier for ultra-low current measurements.

Data were registered on a PC work station and plotted real-time by means of the Labtracer software (www.keithely.com). To realize the measurements, the two sensor pads were connected to the terminal probes of the Source Meter.

Currents were measured before and after nano-gaps opening in order to characterize photolithography and nano-lithography results. Then, they were applied to detect nano-gap closure after the hybridization of target DNA.

3. Results and Discussion

3.1 Fabrication

Compared to other fabrication processes so far explored for nano-gaps electrodes, such as electro-migration [16], electro-plating [17, 18], mechanical-stress [19], the approach based on lithography displays some unique advantages. Standard photolithography allows obtaining in a straightforward manner, arrays of micro-patterned circuits on a huge variety of materials with high reproducibility of patterning details in the array, and between different arrays, thanks to the parallel processing of many copies at once. Reproducibility of the array, besides reduced time of processing, use of materials and equipment, allowed exploiting photolithography for mass-scale production of microelectronic devices.

On the nanometer scale, lithography is more complex, and involves processes which are still expensive, whether in terms of time than of the specialized work required. Although this, it represents a powerful tool to fast engineer versatile nano-gap electrodes systems [20]. The array embedding vertical nano-gap electrodes used in this work was patterned by means of UV photolithography on a metalized SOI wafer.

The resulting electrical pattern was revealed after gold etching, followed by etching of the underlying titanium layer. Then, we used a second photolithography in order of protecting pads, and auxiliary microelectrodes, during SiO_2 sputtering, which served to deposit a nano-metric thickness of the isolating material on the overall structure. This was

done in order of reducing the impact of parasite currents, and leakages, in addition to avoid attachment of biomolecules outside nano-gap electrodes. The micrometric squared pads for the electrical connections, and the auxiliary micro-electrodes, were finally opened by a lift-off process, in which the chemical attack of unexposed photoresist, underlying SiO_2, makes it possible to remove the isolating layer at desired locations. Then, nano-gaps were milled with an average size of about 50 nm by FIB nano-lithography. Results of the fabrication, characterized by means of different optical techniques, and by electrical measurements are included in figure 2.

The interferometer characterization of figure 2 (a) allows to have a three-dimensional view and to visualize layers height, and material homogeneity of the fabricated nano-device. The microscopic image presented in figure 2 (b) shows connection paths for two auxiliary electrodes, labelled as RE and CE, faced at half distance of the pattern in which nano-gap are thereafter milled.

After FIB milling, nano-gap electrodes were cleaned and the size of nano-gaps were characterized by SEM. A sample high-resolution image obtained is depicted in figure 2 (c), showing a gap with an opening of 52 nm.

Well defined patterns, both on the micro and on the nanoscale can be appreciated by the above analysis, and validate the processes used as a fruitful strategy for nano-gap electrodes array fabrication.

Finally, we characterized the fabrication results in terms of the accessibility of produced nano-gap electrodes for electrical bio-detection applications, where high-resistance of bare nano-gaps is a mandatory requirement. For this purpose, we measured current-

voltages characteristics of cleaned nano-gaps at room conditions and in DDI water (18.2 MΩ.cm at 25^0C). The absence of conductivity, as it is shown in I-V curves of figure 2 (d) below the pA range, rules out the possibility of nano-gaps contamination with metals or ions during the fabrication process. This could, in fact, arise both for the re-deposition of milled materials inside nano-gaps, and for the doping of the SiO_2 substrate by the implantation of Ga^+ from the ions beam of the FIB.

Lower resistivity values are measured in the moisty environment provided by milliQ water nano-gap filling, however it accounts for a slight conductivity increase of 10% with respect the previous case. This assures the viability of the nano-gap for low conductance measurements applications.

3.2 Random self-assembling of OPs

We used fabricated nano-gaps electrodes for surface modification by two different thiolated OPs, which could be any other molecular probes provided with a gold-friendly linker. This application is of general and basic interest for the development of nano-gap electrodes for bioelectronics and biosensors. Sensor oligonucleotides are assembled at the gold electrode surface by exploiting the affinity of the thiol group for gold atoms, which interacts strongly, bringing robust and stable monolayers of DNA probes on the gold surface. In the case of nano-gap is required the attachment of two oligonucleotide probes selective to each target edges. In the random self-assembling, a mixture of the two OPs is incubated overnight with the nano-gap and both OPs are attached on each side of the nano-gap. Thus, the probability of attaching OP1 molecules opposite to the OP2 on the other side of the gap plays a role in the success of the target hybridization. Although, by means of this method we do not have all the OPs faced to its counterpart, this is an easier functionalization method for this type of device. Immersion of the gold

substrate in a dilute solution of thiolated molecules at room temperature for few minutes, results rapidly in dense surface coverages. Reorganization process is slower requiring hours to optimize packaging with respect SAM defects.

To characterize the electrodeposited layer of OPs, we adopted electrochemical analysis by applying CV measurements. Simple, and sensitive, CV based surface analysis has been largely applied for micro and nano-electrodes characterization. This method relies on the fact that an intervening molecular layer, assembled at the WE surface, has the effects of a barrier which obstructs the access of the redox solution towards the electrode surface. This affects the electron transfer rate which results in a decrease of the electrode current, as can be easily visualized by reduction of peaks area and height of CV plots.

The parameters employed in CV experiments were optimized so that the molarity of the redox solution used is the lowest at which we could detect clear redox peaks of the cycled species in all the tested nano-gaps electrodes, and in a voltage window safe against etching of both gold and biomolecular probes from the WEs surface.

CV measurements were carried out in 5 mM $K_3[Fe(CN)_6]/K_4[Fe(CN)_6]$ solution by using the electrical configuration represented in figure 1. RE, and CE connections to the potentiostat were kept fixed, while that of WE were interchanged between WE1 and WE2. OP's immobilization or equivalently the bio-functionalization of nano-gap electrodes was characterized by measuring CV of one, and then of other WE that defines the nano-gap, after surface functionalization (figure 3).

Being the peak current determined by the rate of the electron transfer of a diffusional mediator at WE surface, we postulated that modifications arising by self-assembled monolayer should affect the value of the limiting currents measured inside the electrochemical cell.

For a reversible electrochemical process, with fast electron transfer, the value of the peak-to-peak potential is expected to be about ΔE_p= 57 mV and the ratio between cathodic and anodic current equal to 1. Variations from these values indicate departures from the reversible behavior which are in general caused by either slow electron transfer kinetics and chemical reactions of the oxidant/reducing species, which makes the rate of electron transfer becomes comparable to the rate of mass transport [21]. In such cases, the electrochemical reaction requires over-potentials and peak heights occur at greater potentials, as it is observed in our case.

The peak-to-peak potentials difference and the oxidation to reduction current ratio were used to characterize the surface modification and to understand the electrochemical properties of the studied system.

According the above, the quasi-reversible system observed with bare gaps become irreversible after oligonucleotide functionalization. The adsorbed interface on the electrode gap slows down electron exchange with a clear increase of the peak-to-peak potentials observed.

Empirical values were used also to characterize nano-electrodes functionalization, by assuming that modifications arising by self-assembled monolayer affect the value of the limiting currents measured inside the electrochemical cell and so give us information about the properties of the liquid/electrode interfaces considered. Accordingly, we de-

fined surface coverage percentages by the relative decrease of limiting currents at WEs due to OPs immobilization;

$$\Delta I/I_{max}[\%] = \frac{I_{peak}(OP1;OP2) - I_{peak}(bareWE1;bareWE2)}{I_{peak}(bareWE1;bareWE2)} \times 100$$

Where $I_{peak}(OP1;OP2)$ is the height of the current peak measured after immobilization of one of the OPs, while $I_{peak}(bareWE1;bareWE2)$ is the height of the current peak measured on cleaned electrodes, before carrying out any immobilization. Percentages values calculated in this way are not representative of absolute surface coverages, but are useful to compare results.

Reduction of peak current values ranging between 70% and 90%, is consistent with high degree of molecules immobilization on WE surface, which are providing an obstacle to redox solution diffusion toward electrode area. Mainly, this is helped by electrostatic repulsion of the negative charges of DNA and the negative ferrocyanide molecule. Decrease of ferrocyanide electron transfer rates are visually reflected by flattened CV shapes.

3.4 Electrophoresis assisted site selective immobilization of OPs.

As we already commented in the introduction, available methods allowing bio-receptors delivering such as inkjet or contact printing are well-tailored for micrometric arrays, but are difficult to exploit at the nano-metric distances and /or vertical electrodes typical in nano-gap devices. For this latter situation alternative methods, initially developed for DNA microarrays, such that based on electrophoretic effects which polarizable molecules undergo in presence of an applied electrical field, have been developed. Although, compared with DNA microarrays, the problem addressed here presents some substantial difficulties namely: the nano-metric distance between the two electrodes which are moreo-

ver, placed on a vertical plane, and the high electrical field strength that can reach nanometric structures, even at low applied voltages.

We used electrophoretic driving of the OPs inside the nano-gap electrodes by applying an external voltage in order to promote the formation of two specific self-assembled-monolayers (SAMs) at the selected nano-gap electrode surface. To do this, we applied a DC signal of 1V of amplitude for 60 sec. between one of the two WEs (+) and the auxiliary CE (-), meanwhile spotting a solution containing one of the two OPs, which is thereafter rapidly removed and thoroughly cleaned (figure 4).

By doing so, we expected to attract the short negative probes, which are delivered independently, toward the nano-gap electrode positively charged. In this way we hope to improve the selectivity of the OP's monolayer at the chosen surface with respect to spontaneous absorption due to solution diffusion at the electrode surface. The parameters used were established on the basis of existing literature, in particular in [10, 12, 13, 14, 15]. Nevertheless, we exploit milder conditions compared to the above works, because we deserve concerns on the use of test voltages greater than 1-2 V in nano-gap electrodes. Indeed, after establishing reference parameters through literature, the final ones used where optimized in a series of experiments in which the effects of different voltages and buffer solution were tested.

For this latter purpose, a DC signal with voltage varying between 0.2 V and 1 V was applied between CE (-) and WE1 (+), while incubating the nano-gap with a solution of OP1 either in 60 μM of histidine or DDI water. Results obtained are shown in figure 4(a) and 4(b), demonstrating that maximum surface coverage is obtained after application of 1 V and in DDI water. This latter result is especially surprising because in the case of microelectrodes a conductive buffer is usually advantageous for DNA electrophoresis. It would

be interesting to investigate further this point and to relate it with nano-gap dimensions, but it is beyond the aim of this work. Once optimal parameters were determined, we carried out electrophoresis assisted immobilization of oligo-probes by applying the 1 V DC signal between CE (-) and WE1 (+) in presence of OP1 solution in DDI water. After cleaning, a CV characterization of OP1's adsorption on WE1 and WE2 (selectivity control) was performed following the same method explained in 3.2. A second (reversed) DC signal was applied between CE (-) and WE2 (+) while spotting the solution of OP2, followed by CV characterization of both electrode; in WE2 was tested the coverage with OP2 and in WE1 was studied the stability of the already attached OP1 after 1V applied on the neighbor electrode. Results obtained are shown in figure 4.

According to the behavior observed here, the application of a positive DC signal on a given WE(1,2) when the corresponding OP(1,2) solution is in the nano-gap, affects ferrocyanide/ferricyanide CV response, both in current peak/area values, and in increased distance between reduction and oxidation peaks. Both effects are due to the decrease of electron transfer of ferrocyanide/ferricyanide at the OP modified nano-gap electrode surface. From obtained results, we conclude that OPs are successfully attached at the nano-gap electrodes surface by means of electrophoresis.

It is important to remark the selectivity of this electrophoretic immobilization. In fact, the first DC pulse, under which WE1 is positively charged, has no effect on the bare WE2, as it is verified by measuring the same initial CV observed before DC application. Moreover, the electric field induced to generate a positive charge on WE2 has no effects on the OP1 molecular layer previously immobilized on WE1, where an unaltered voltammetry behavior is measured after the second immobilization step.

Similar percentage of covering is observed in the two sides of the nano-gap after two different electrophoretic driving of OP1 to WE and OP2 to WE2. The successfully drive of OPs to the specific WE is demonstrated by the decrease of current observed in the CV characterization, which is related to 20-18% of surface coverage. Moreover, a low decrease of coverage is observed in WE1, after the application of the electric field required for the functionalization of WE2 with OP2. Although, being only 4% of CP1 coverage affected by the application of electric field on the neighboring electrode, this method demonstrates potentiality as tool for the selective addressing of molecular probes in nano-gaps devices.

In general, lower surface coverages are obtained following this latter process, comparing with the 70-90 % of surface coverage observed in random adsorption, but a drastic reduction of immobilization times, from overnight incubation, required by all previous methods, to the overall 5 minutes which are necessary to accomplish electrophoretic driving of oligo-probes, is achieved.

So, the method proposed demonstrates potentiality as tool for the selective addressing of molecular probes in nano-gap electrodes devices. However, if we compare these results with that obtained from random assembly of OPs represented in figure 3, we observe a more drastically reduction, both of peaks current and of the overall CV area.

The immersion of a gold substrate in a dilute solution of adsorbates at room temperature for few minutes results in dense surface coverages. Although, it is well-known that reorganization process is slower requiring hours to optimize packaging with respect SAM defects. This could be at the basis of the remarkable difference observed between surface coverages of nano-gap electrodes functionalized by random assembly of OPs with that assisted by electrophoresis.

3.5 Target hybridization with random and site selective functionalized nano-gap

To get more insight on the quality of the assembled SAM and their usefulness in application, we considered the capture of a target ssDNA which is complementary, end-to-end, to the last 20 bases of the anti-symmetric OPs of each sides of the nano-gap. The hybridization of the DNA target with the two OPs attached to each side of the nano-gap, link the gap and so close a circuit between the current source and the drain. It has been largely shown [22] that the current through nano-gap electrodes connected by a well-suited DNA wire is substantially greater with respect the unconnected cases.

Considering this, we measured the current through nano-gap electrodes with randomly, and selectively assembled OPs, after one-hour incubation with the TG-DNA which connects the edges of the devices through interaction of complementary base-pairs. These values were normalized with respect the current measured after functionalization with the bio-receptors. The results obtained are shown in figure 5.

Here we plot the relative increase of nano-gaps current measured after hybridization with the complementary ssDNA for randomly assembled and electrophoresis driven OPs. We detect a clear increase of nano-gaps current independently from the method used for the bio-functionalization of the electrodes. Although for all applied voltages, we measured greater currents at nano-gaps with randomly assembled oligo-probes. We postulated that it could arise in virtue of the poor surface coverage achieved by site-selective bio-functionalization, so that there is a lower probability of a successful hybridization compared to the randomly assembled case. We cannot infer only from this results on the influence of voltage application on the integrity of the OPs and their ability to capture the complementary DNA.

4. Conclusion

We analyzed the effects of different methods of bio-functionalization with DNA in nano-gap electrodes system useful for biosensing and for general bioelectronics purposes. Nano-gaps are usefully improved for electrical transduction of bio-molecular interaction, as well as building blocks for molecular electronics circuits being characterized by an easy integration with lab-on-chip final package, and naturally tailored for direct electrical detection. Functionalization of such nano-devices is a relevant issue to assure its optimal performance.

The effects produced by different functionalization methods were considered in the case of a practical application of the fabricated nano-gap electrodes aimed at hybridization detection by a switch on current system, where DNA target close a current circuit in the nano-gap. Capture probe functionalization of the two faced electrodes of the nano-gap was performed by means of two methods; first a random self-assembling of a mixture of OP1 and OP2 and second, controlling the positioning of two different OPs inside the nano-gap electrodes system, by applying a DC signal between one WE in the nano-gap and the CE provided in its proximity. Results from this selective method of bio-functionalization were compared with random assembly of OPs in terms of surface coverage of nano-gap electrodes based on electrochemical analysis. The latter method gave rise to denser OPs SAM which resulted in increased hybridization efficiency, as shown by the higher nano-gaps current observed after addition of a complementary target in these devices.

5. Acknowledgments

This work was funded by the project OLIGOCODES from the Spanish Ministry of Economy and Competitiveness MAT2012-38573-C02. The Nanobioengineering Group has support from the Commission for Universities and Research of the Department of Innovation, Universities, and Enterprise of the *Generalitat de Catalunya* (2014 SGR 1442). CIBER-BBN is an initiative funded by the VI National R&D&i Plan *2008-2011, Iniciativa Ingenio 2010,* Consolider Program, CIBER Actions and financed by the *Instituto de Salud Carlos III* with assistance from the European Regional Development Fund.

6. References

[1] Zaffino, R.L., Galan, T., Pardo, W.A., Mir, M., Samitier, J., *WIREs Nanomed Nanobiotechnol* 2015, 7 (6) 817-827.

[2] Nair, P.R., Alam, N.A. *Applied Physics Letters,* 2006, **88** (23), 233120-233123.

[3] Xing, C., Guo, Z., Yang, G.M., Li, J., Li, m:Q., Liu, J.H., Huang, X.J. *Materials Today,* 2010, **13** (11) 28–41.

[4] Somenath, R., Chen, X., Li, M.H., Peng, Y., Anariba, F., Gao, Z. *Journal of the American Chemical Society,* 2009*,* **131** (34) 12211–12218.

[5] Wei, S., Deng, H., Ren, Y., Gao, Z. B*iosensors & Bioelectronics,* 2013, **43**, 165–172.

[6] Mir, M., Dondapati, S.K., Darte, M.V., Chatzichristidi, M., Misiakos, K., Petrou, P., Kakabakos, S.E., Argitis, P., Katakis. I. *Biosensors and Bioelectronics*, 2010, **25** (9) 2115–2121.

[7] Ruiz, S.A., Chen, C.S. *Soft Matter*, 2007, **3**, 168-177.

[8] Piner, R.D., Zhu, J., Xu, F., Hong. S. *Nanolithography*, 1999, **283**, 661–664.

[9] Benavidez, T.E., Torrente, D., Marucho M., Garcia, C.D. *Langmuir*, 2015, **31** (8), 2455–2462.

[10] Heller, M.J. *Annual review of biomedical engineering,* 2002, **4**, 129-153.

[11] Endres, R.G., Cox, D.L., Singh. R.P. *Cond. Mat. Soft*, 2008, **20**, 1–12.

[12] Porath, D., Bezryadin, A., Vries, S., Dekker, C. *Nature*, 2000, **403** (6770) 635–638.

[13] Braun, E., Eichen, Y., Sivan, U., Ben-Yoseph M. *Nature*, 1998, **391** (6669) 775–778.

[14] Welch, K., Blom, T., Leifer, K., Strømme, M. *Nanotechnology*, 2011, **22** (12) 125707-125713.

[15] Anton, K., Yurke, B., Toppari, J.J., Linko, V., Törmä, P. *Small, 2008,* **4** (4) 447–50.

[16] Lambert, M.F., Goffman, M.F., Bourgoin J.P., Hesto, P. *Nanotechnology*, 2003, **14** (14) 772–777.

[17] Yoshiaki, K., Nakashima, H., Furukawa, K., Torimitsu, K. *Thin Solid Films*, 2003, **438-439**, 317–321.

[18] Yann-Vaï, K., Kubatkin, S. *Small, 2009,* **5** (22) 2541–2544.

[19] Tao, L., Hu, W., Zhu, D. *Advanced Materials,* 2010*,* **22** (2) 286–300.

[20] Takashi, N., Kubota, T., Mashiko, S. *Thin Solid Films*, 2003, **438-439**, 374–377.

[21] Brownson, D. A. C., Banks, C. E. The Handbook of Graphene Electrochemistry, Springer-Verlag, London 2014, pp. 35-44

[22] Zaffino, R.L., Pardo, W.A., Mir, M., Samitier, J. Biosensors at the Nanoscale in *Biosensor and Cancer* edited by Victor R. Preedy, Vinnod Patel, 2012, 62–84.

Fig. 1 Schematic of the electrical circuit used to connect nano-gap electrodes to the measurement unit. Blue pattern is covered by SiO_2. In the zoom, it is shown a cartoon illustrating the nano-gap electrodes. The two gold electrodes of the nano-gap are functionalized with two different OPs, useful to capture a specific target.

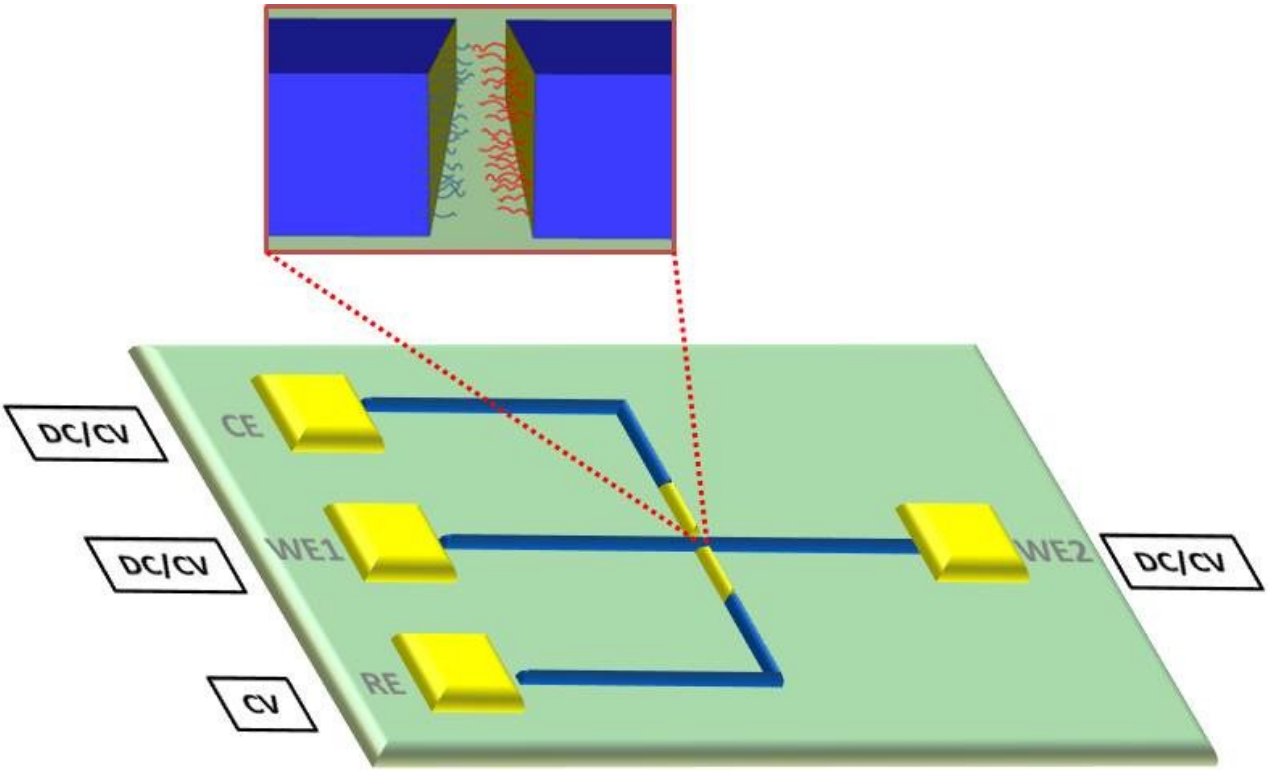

Fig. 2 (a) White light interferometry picture of the electrode pattern before nano-gap milling. (b) Optical microscopy image of the electrodes patterning after photo-lithography. (c) SEM image of a nano-gap after FIB milling and cleaning processes. (d) I-V characteristics of nano-gaps measured after cleaning, in the inset I-V curved measured before nano-gaps milling.

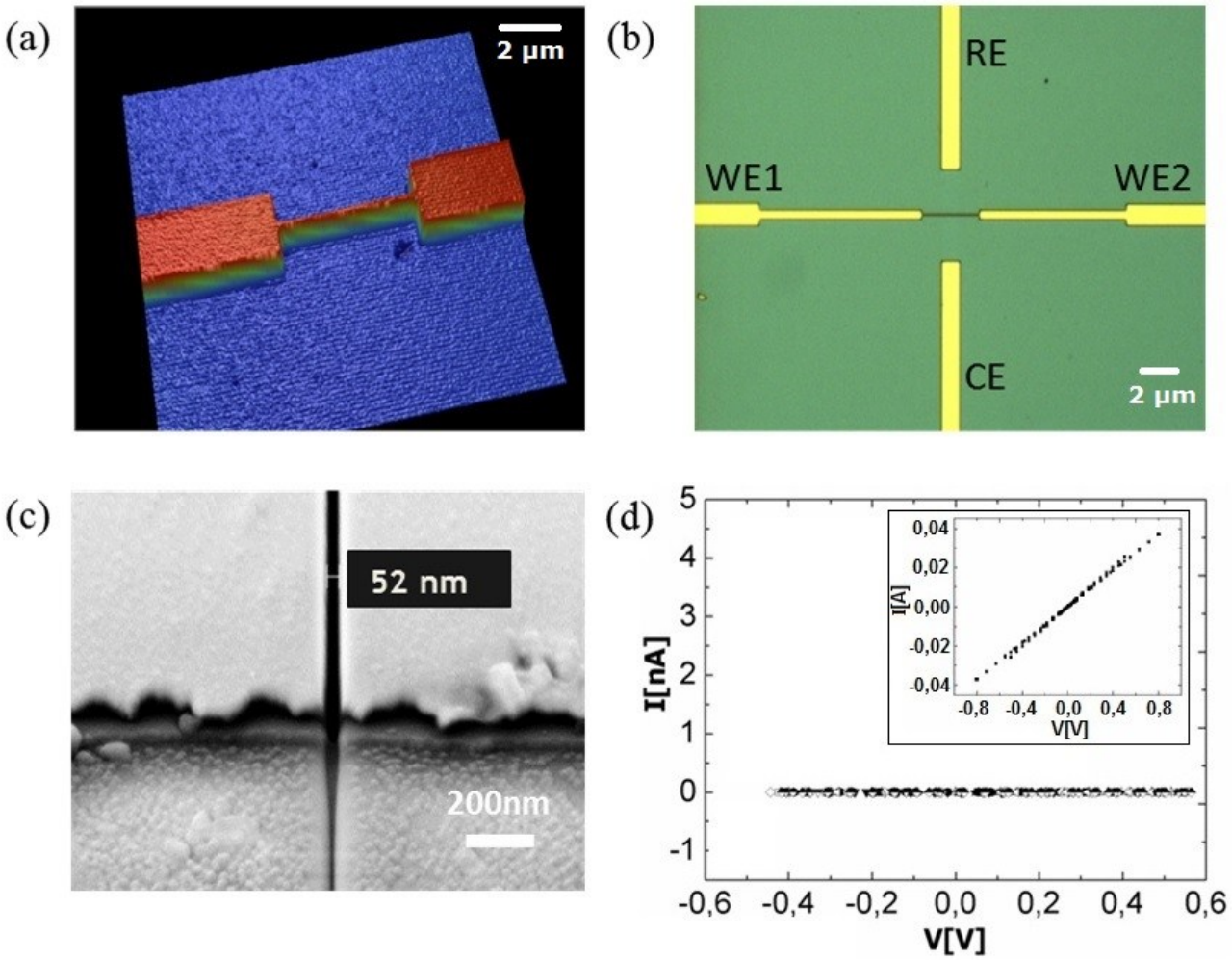

Fig. 3. CV obtained at WEs of nano-gaps before and after overnight incubation with a random self-assembling of OPs.

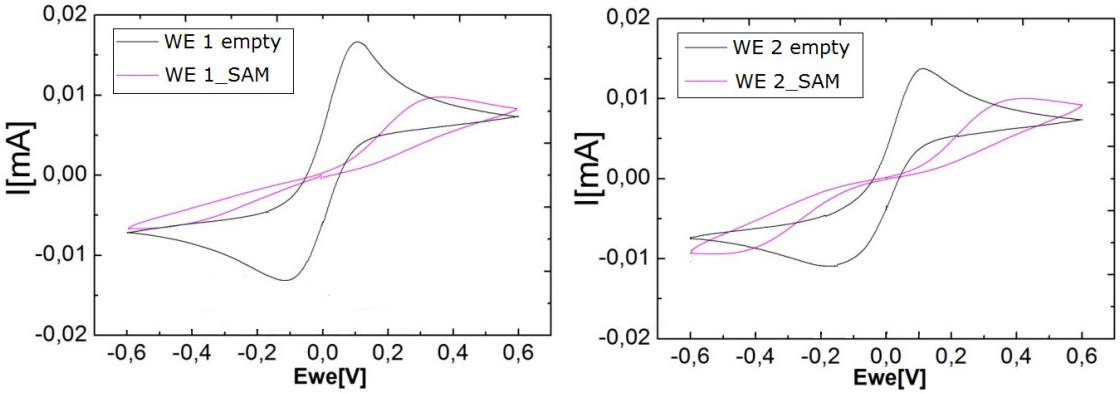

Fig. 4 (a) Surface coverage after application of different DC voltage values for 60 sec. (b) Surface coverage in histidine and DDI water at 1 V for 60 sec. (c) and (d) Results of the electrochemical characterization of site selective deposition of OP1 in WE1 (left) and OP2 in WE2 (right). (n = 3) OP1 at WE1 is the coverage after 60 sec. at 1V with OP1 in WE1. Stability control is the coverage of OP1 functionalized WE1 after 1V for 60 sec. with OP2 at WE2. Selectivity control is the coverage of the non-functionalized WE2 after 1V for 60 sec. with OP1 at WE1.

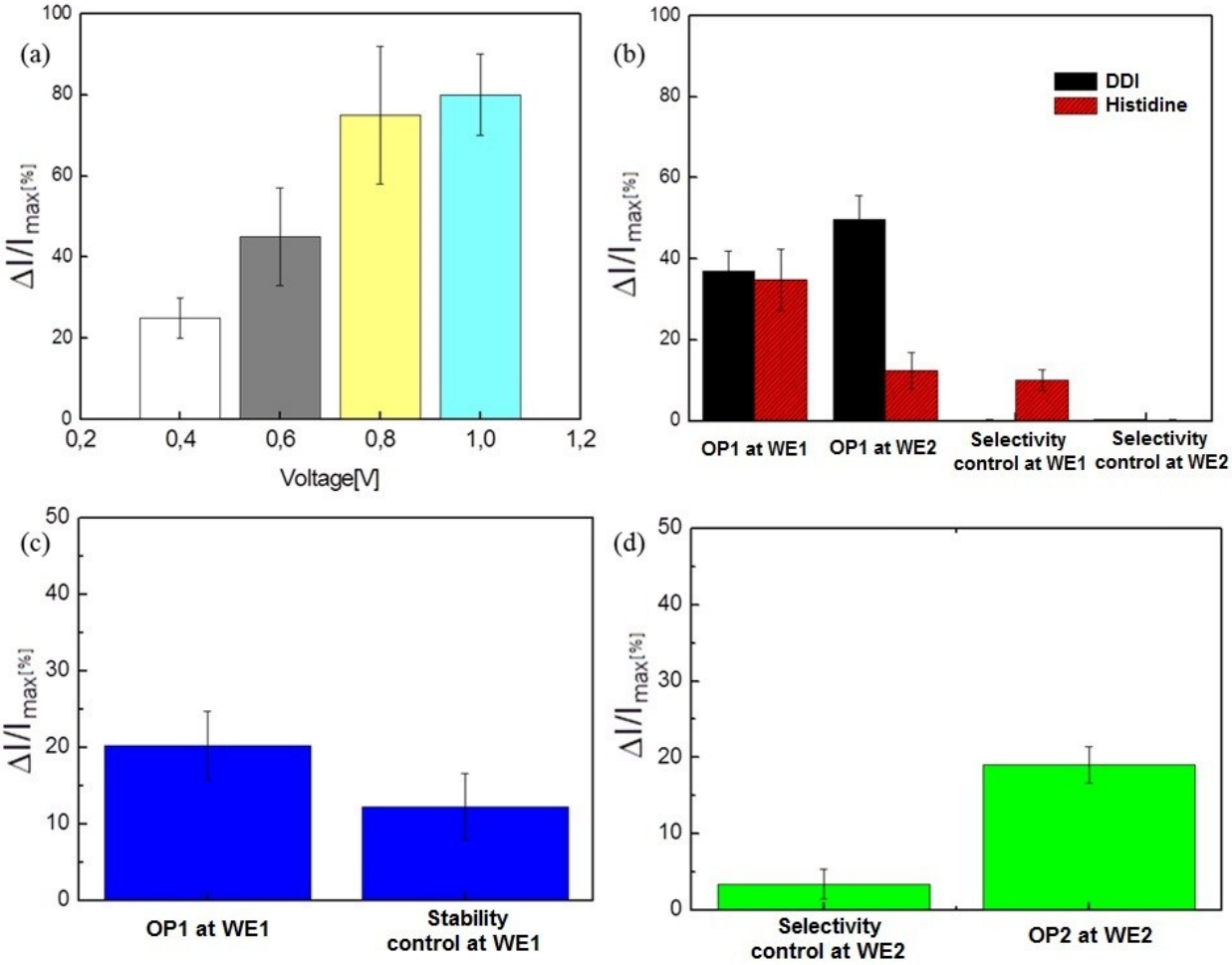

Fig. 5 Relative increase of nano-gaps current after hybridization of a complementary DNA target for randomly assembled and electrophoresis driven oligo probes. Test-voltatge at 0.4 V. (n=3)

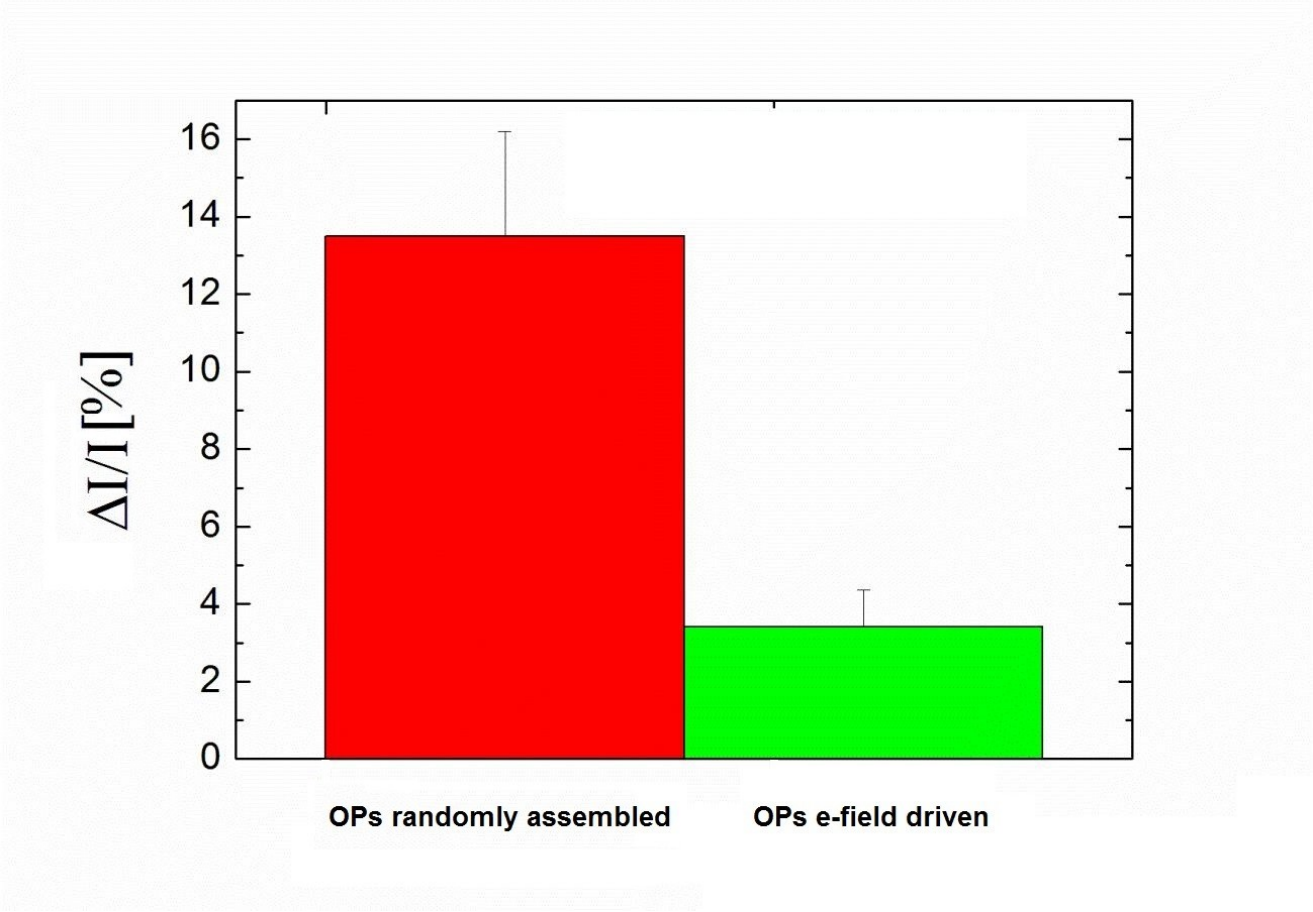

Tab.1 Experimental values of the peak-to-peak potentials and the ox/red current ratio.

WE	ΔE_p (bare)	I_p^{ox}/I_p^{red}	ΔE_p (SAM)	I_p^{ox}/I_p^{red}
WE1	194±4 mV	1,11	740±5mV	1,14
WE2	245±8 mV	1,23	830±6mV	1.12